Performance assessment of a reversible Tesla machine

Ravi Nath Tiwari [1,*], *Alberto* Traverso[1], and *Federico* Reggio[2]

[1]University of Genoa, DIME, 16145 Genova, Italy
[2]SIT Technologies s.r.l., 16121 Genova, Italy

Abstract: It is well known that bladeless or Tesla turbomachinery, which was invented by Nikola Tesla in 1913, has several distinct features, such as reversibility of operation, which includes expander as well as compressor operation, just by reversing the rotational speed, provided that the statoric channels are purposely designed. Despite their potential application to a variety of fields, such as energy harvesting, automotive, light aircraft, and food processing, especially for low volumetric flows, Tesla machines have not found yet a specific market niche. In fact, at small size, it is estimated that the Tesla machinery does not change performance significantly, while conventional bladed machines are subject to significant efficiency reduction because of mechanical tolerances, thus matching the Tesla relatively low performance. Therefore, Tesla machines can become the fluid machinery of choice for small-size applications, thanks to their competitive performance at that size, simple construction, and reversible operation. A key objective of this paper is to numerically study Tesla devices in both expander and compressor modes with air as the working fluid. As a consequence of the high losses due to rotor and stator interactions, statorless (volute) configurations are investigated here, showing superior performance in both direct and indirect modes of operation. With reference to a laboratory prototype under construction, this paper presents the numerical design results, which predict the peak isentropic efficiencies of 63.5% and 57.5%, for the expander and compressor mode of operation, respectively. Actual prototype is expected to match those performance, apart from leakage and ventilation losses, not included in the numerical analysis.

Nomenclature

E_k	Ekman number [-]	N	Rotational speed [krpm]
Eff.	Efficiency [-]	p	Pressure [Pa]
h	Half disk gap [mm]	P	Power [W]
k	Specific heat ratio [-]	r	Radius [mm]
$\dot{m}$	Mass flow rate [g/s]	R_e	Reynolds number [-]
n	Number of disk gaps [-]	RT	Rotor [-]

* Corresponding author: ravinath.tiwari@edu.unige.it

t Disk thickness [mm]
T Temperature [K]
TC Tesla compressor
TE Tesla expander
VT Volute model [-]

Greek Symbol

β Pressure ratio [-]
δ Boundary layer thickness [mm]
ε expansion ratio
η Efficiency [-]
τ Torque [Nm]
ν Kinematic viscosity [m^2/s]
ω Angular velocity [rad/s]

Subscripts

i Inlet
o Outlet
t, t-t Total, total to total
st, t-st Static, total to Static

1. Introduction

Tesla filed patents for bladeless pumps and turbines in 1909 and 1911 based on the boundary layer principle. The patents were both accepted in 1913 [1][2]. Due to Tesla's invention of the bladeless turbine and pump, the technology is known as Tesla-type turbomachinery. Nowadays there is a high demand for affordable, efficient, compact, reversible, and low-noise devices at small scale. Such market requirements can be met with Tesla or bladeless technologies[3][4]. There are several advantages to this turbomachinery concept, which include reversible operation, low cost, affordable for use with dirty fluids, and low noise levels compared to conventional devices [3][5][6][7][8][9][10]. A Tesla machine has thin disks mounted on the shaft with gaps or spacers, and this disk assembly (rotor pack) is called the Tesla rotor. As shown in Figure 1, the entire rotor assembly is mounted into a cylindrical volute casing with a locking plate, which is mounted with a bearing to hold the shaft in place. In compressor mode (indirect mode) fluid enters axially at the inlet, flows spirally through the disk gaps, and leaves radially through the volute: overall, the machine provides energy to the fluid, absorbing mechanical energy from the shaft. When the Tesla turbine is operated in the opposite direction, i.e., direct mode of operation as expander, the flow direction is reversed, as well as the angular speed: as a result, pressure head is transformed into mechanical energy, that can be extracted from the rotating shaft.

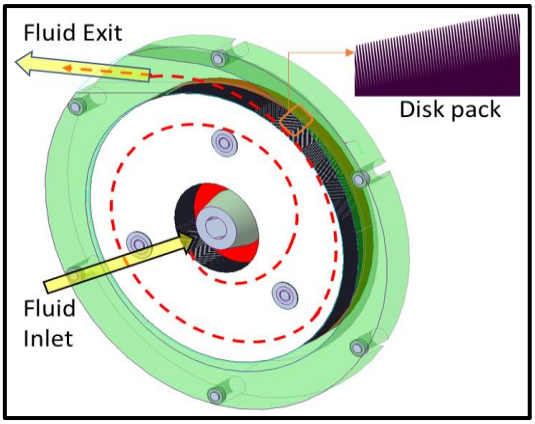

Figure 1: Reversible Tesla machine (compressor mode): principle of operation.

Rice was a leading researcher in Tesla technologies, who stated that conventional devices performance degrades when scaled down, while Tesla machine performance remains almost constant [5]. There were 77 disks in Rice's bladeless rotor for the Tesla compressor, with an outer radius of 75 mm, a disk thickness of 0.5 mm, and a disk gap of 0.5 mm each. The experimental results indicate a 23% efficiency at 20000 rpm and a mass flow rate of 101 g/s,

whereas the compressor was designed for 30000 rpm, not reachable because of mechanical issues. Bladeless technologies have not been sufficiently researched, performing less than conventional devices. Due to the global focus on low pollutants, low costs, low noise, compactness, lightweight, and efficient technologies at small scale, bladeless technologies experienced exponential growth in research at the turn of the 20th century [6][8]. There is a possibility that Tesla technologies could be considered as an alternative to micro-conventional turbomachinery. In niche markets, there are several Tesla-type turbomachinery opportunities, for example, Tesla pump, blood pump, and expander. Tesla-type pumps are currently available worldwide for micro applications. However, further research is needed to make the system reversible and efficient. University of Genova spinoff company (SIT technologies Srl) showed interest in such technologies and developed many prototype models [11]. The 3-kW air expander was designed with an outer diameter of 120mm, 0.1 mm disk thickness and a gap, achieving 36.5% iso-entropic efficiency, highest ever recorded experimental efficiency with air as working fluid, while numerical analysis indicated 58% without any assembly loss [8]. The loss characterization of this device was demonstrated to show a great impact of end-wall leakage and ventilation losses [12]. Tesla technologies can function as both an expander and compressor without requiring any significant modifications. To verify the reversibility of this 3-kW expander, Tiwari [6] numerically simulated it in compressor mode and compared the results experimentally with different rotational speeds. A pressure ratio of 1.15-1.25 was measured at 20000 rpm and 30000 rpm, which indicates that the prototype can function as a blower [6]. Additionally, this model was examined experimentally for its acoustic features, comparing against a conventional bladed blower [3]. The vibro-acoustic analysis demonstrated, for the first time, that bladeless devices can significantly outperform bladed devices, having much lower levels of noise emissions.

To achieve the best performance, disk gap should be three times the thickness of the boundary layer, with Ekman numbers (E_k) around 1.5-1.6 and Reynolds numbers (R_e) 9-11 [13]. According to Tiwari's numerical results, the disk diameter ratio should be between 2.5 and 4.5 in order to achieve the best possible efficiency in compressor mode. With a larger diameter, efficiency increases at a low mass flow rate but decreases with a high gradient when the mass flow rate increases [14].

A reversible Tesla machine is described in this paper with the following assumptions.

- In order to achieve the best rotor performance, in compressor mode, there is an optimal disk gap as determined by Ekman's (Ek-1.5-1.6) and Reynolds' (Re-10-11) numbers, as well as a disk diameter ratio of 2.5-4.5.
- A volute (VT)-shaped casing is considered because it can easily allow reversible flow operation, as bladeless diffuser or nozzle/distributor.
- To avoid inlet losses (exit losses in the expander), a wide inlet section is considered.
- Analyses are conducted for reversible operation (compressor and expander) and performance is compared for both modes of operation.

2. Numerical Investigation of Tesla reversible machine

This section examines the numerical analysis of a bladeless and statorless reversible machine in 3D CFD, which captures the most relevant flow phenomena that occur inside a Tesla (bladeless) compressor and expander. The machine is designed specifically for compressor use, however because of Tesla reversibility advantages, it can operate also in expander mode.

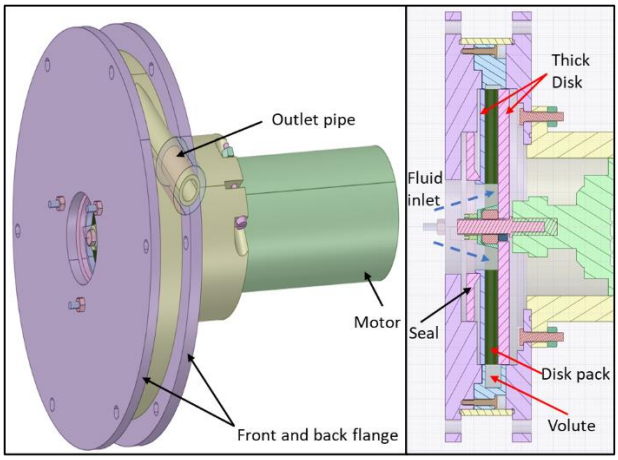

Figure 2: Reversible Tesla machine: 3D and cross-sectional view.

The performance of a reversible bladeless compressor is numerically analyzed with an optimal rotor and volute design in order to maintain sufficient accuracy with minimal computational effort. A reversible Tesla machine 3D model and cross-sectional view are illustrated in Figure 2, which contains a 0.1 mm thin disk (t) as well as a 0.3 mm disk gap (2h). This rotor pack has a total length (l) of 8 mm where the number of disk gap (n) is 20, presenting thick end disks for structural integrity. Since the prototype model is in the process of being constructed, this paper presents numerical results of such machine, in both direct and indirect operational modes, s without considering assembly losses, namely end-wall ventilation and leakage losses, mechanical losses. A high leakage was observed in early Tiwari's study, so sealing systems are being considered in the current prototype model to reduce leakage [6].

2.1. Reversible Tesla machine geometry and boundary conditions

Data regarding the Tesla reversible machine geometry is presented in Table 1. It is designed for 22 krpm with a disk gap (2h) of 0.25 mm calculated using the optimal Ekman number (E_k) 1.5-1.6, and a diameter ratio (DR) of 3.2 (160mm/50mm). Since the spacer (2h) with 0.25mm is not readily available, the easiest spacer available with 0.3 mm is going to be used in the prototype model, which is suitable for optimal rotational speed (N) of 17 krpm. Due to this, both gaps (0.25 mm and 0.3 mm) and speeds (17 krpm and 22 krpm) are considered in the CFD analysis. A single domain of fluid is considered for the numerical analysis with a coupled rotor (RT) and volute (VT) as shown in Figure 3. For the numerical analysis in both Tesla compressor (TC) and expander (TE) modes, a single fluid domain is considered with half of the disk gap (h) and half of the disk thickness (t/2). It can be seen in Figure 3 that the boundary condition for a single fluid domain includes symmetry 1 (volute-VT), while the boundary condition for a second fluid domain includes symmetry 2 (half disks gap with volute from center).

There are two faces to the rotating walls in Figure 3, as indicated by the black circles. Figure 3 (I) illustrates boundary conditions for the Tesla compressor with volute (TCVT3), while Figure 3 (II) illustrates boundary conditions for the Tesla expander with volute (TEVT3). The TCVT3 and TEVT3 is the model's name of the Tesla compressor and expander respectively for rotor diameter ratio 3. Despite the difference in rotational direction, inlet and outlet, all boundary conditions are the same in both conditions.

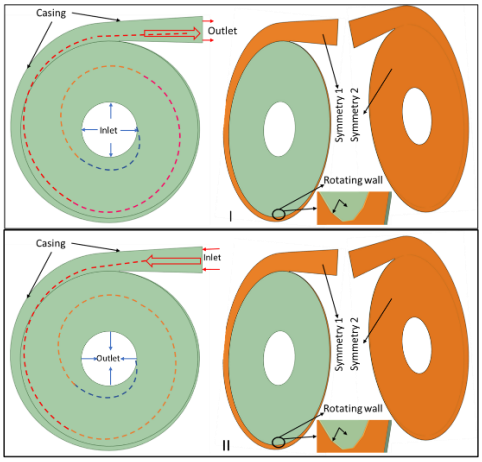

Figure 3: Reversible Tesla machine geometry, and boundary conditions (I) compressor mode (TCVT3), and (II) expander mode (TEVT3)

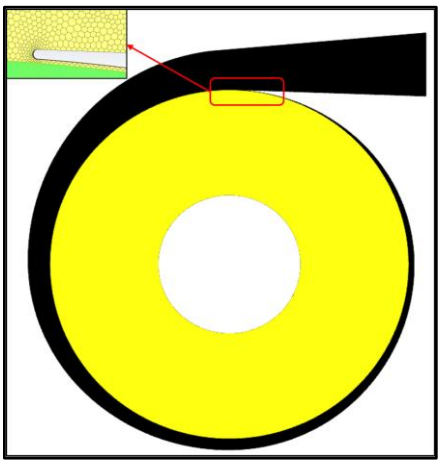

Figure 4: Reversible Tesla machine: generated mesh

Table 1: Design parameters of reversible Tesla or bladeless machine

Parameters	Model
Disk outer diameter, mm	160
Disk inner diameter, mm	50
Diameter ratio	3.2
Disk thickness, mm	0.1
Disks gap, mm	0.25, 0.3
Number of disk gap, n	20
Re,$(\omega(2h)^2/\nu)$	9-12
E_k number, $(h\sqrt{(\omega/\nu)})$	1.5-1.8
Volute duct outlet, mm	17
Volute, outer dia., mm	196
Rotational speed N, krpm	22 and 17

Table 2: Grid sensitivity of reversible Tesla compressor

Mesh model #	# Nodes	# Element	Static pressure (Pa)	% Change	Torque (Nm)	% Change	Total Temp. (°k)	% Change
1	3396719	582713	24010	-2.20%	0.00654	-2.21%	333.26	-0.22%
2	3971958	827291	24080	-1.91%	0.00655	-2.11%	333.29	-0.22%
3	6342611	1303646	24115	-1.77%	0.00656	-1.87%	333.4	-0.18%
4	13632783	2698004	24240	-1.26%	0.00666	-0.36%	333.89	-0.04%
5	41434311	7808354	24550		0.00669		334.01	

2.2. Computational setup and grid generation

This study used the commercial software ANSYS FLUENT to solve steady and compressible flows using a pressure-based steady solver for an ideal gas as the working fluid. This numerical study uses the k-ω SST viscous model, a widely accepted industry standard for turbulence analysis, to discretize the three-dimensional Reynolds Averaged Navier–Stokes (RANS) equations. Furthermore, the energy equation is extended to include the effects of heat transfer in the flow field. The viscous heating option is selected in order to take into account the changes in temperature caused by shear forces. A coupled scheme for fluid coupling of pressure and velocity is used to solve the governing equations. For steady-state flows, this scheme provides a robust and efficient single-phase implementation, which performs better than segregated schemes. An upwind linear interpolation scheme based on second-order linearity is utilized in this scheme.

At the compressor inlet, boundary conditions for temperature (300 K) and total pressure (atmospheric) have been set, while the mass flow boundary condition has been set at the outlet [6][14]. While it is in expander mode, the pressure inlet and temperature (300 K) have been set for the inlet, while the boundary condition for the pressure outlet has been established [8]. In both modes, the rotating wall is considered a moving wall with no-slip conditions. A set of inflation layers is applied to both stationery and moving walls. The average facet wall function y+ values are maintained in accordance with the k-ω SST model.

In both compressor and expander modes (coupled rotor and volute), polyhedral meshes are generated as shown in Figure 4. Mesh sensitivity analysis is performed from coarse to fine cells for accurate analysis as shown in Table 2. The coupled rotor-volute configuration generates a tetrahedral mesh, which is converted into a polyhedral mesh by using ANSYS FLUENT software. The use of polyhedral elements has increased in popularity as an alternative to tetrahedral elements. In comparison to a tetrahedral structure, a polyhedral structure has the advantage of having more adjacent neighboring cells. The sensitivity of the coupled rotor-volute configuration is determined by taking into consideration 2698004 cells (second last row in Table 2) with changes in static pressure, torque, and total temperature of 1.26%, 0.36%, and 0.04%, respectively.

3. Results and discussion

A performance analysis is presented in this section for both direct (expander) and indirect (compressor) modes of the reversible Tesla prototype under consideration.

3.1. Reversible Tesla machine in compressor mode

In this section, the performance analysis of the Tesla compressor is presented. As shown in Figure 5 (I), the ratio of total to static pressure (β_{t-st}) is plotted against mass flow rate (22 krpm, 0.25mm and 0.3mm spacers) and 17 krpm, (0.3mm spacers). The total to static pressure ratio is calculated using Eq. (1).

$$\beta_{t-st} = \frac{p_{st-o}}{p_{t-i}} \tag{1}$$

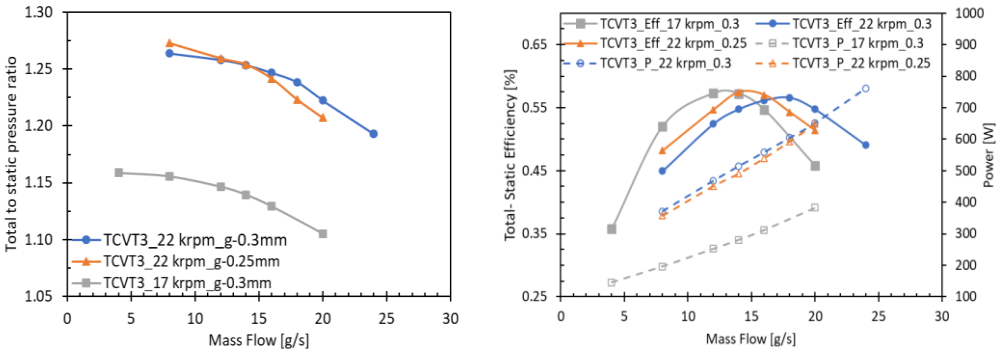

Figure 5: Reversible Tesla machine in compressor (TCVT3) mode: (I) Total to static pressure ratio vs mass flow rate (II) Total to static efficiency (solid line) and power (dashed line) vs mass flow rate.

The pressure ratio (β) at 22 krpm is higher for a 0.25 mm disk gap toward a lower mass flow rate but is slightly lower for a 0.3 mm disk gap. There is a higher pressure of 1.28 at 8 g/s and 1.16 at 4 g/s for 22 krpm and 17 krpm, respectively. It is expected that the absence of rotor blades will avoid the well-known stall phenomenon in bladed compressors at low flow, driving to compressor surge: experimentation will tell how flexible the Tesla compressor will be, being potentially able to operate across a very wide range of mass flows, including very low mass flow conditions. In fact, it seems already that Tesla technologies can prevent surges in accordance with the Rice results [5]. As shown in Figure 5 (II), the total to static efficiency (η_{t-st}) of a Tesla compressor is plotted against the mass flow rate on left y axis (solid line)

while inlet power on right y axis (dashed line). The total to static efficiency is calculated using Eq (2), where k is specific heat ratio, ṁ is mass flow rate and Tti is total inlet temperature. The inlet power is calculated using Eq. (3) where τ is torque and ω is angular speed. The specific heat at constant pressure, cp, and the heat capacity ratio, k, are considered constant with temperature. Cp = 1.006 kJ/kg K and k = 1.4 are used for air.

$$\eta_{t-st} = \dot{m} * C_p * T_{t_i} * \left(\frac{\beta_{t-st}^{\left(\frac{k-1}{k}\right)}-1}{\tau*\omega}\right) \quad (2)$$

$$P_{cfd-in} = \tau * \omega \quad (3)$$

It is found that the total to static efficiency reaches the top value of 57.5 % in the 12-14 g/s mass flow interval for optimal disk gap of 0.25 mm with rotational speeds of 22 krpm. On the other hand, the efficiency for the 0.3 mm disk gap at 22 krpm is 56.5% at 18 g/s. As a result of a bit higher disk gap, the surface area increases, which in turn results in a greater mass flow rate, but efficiency is reduced by 1% since the disk gap isn't optimal. At this condition, the inlet power ($P = \tau * \omega$) is approximately 600W at peak efficiency and 500W at peak efficiency for the 0.3 mm gap and 0.25 mm disk gap, respectively. From a low mass flow rate to a higher mass flow rate, both power curves increase linearly, but the power curve for the 0.25 mm gap is a bit lower, indicating a slightly higher efficiency. In general, the optimal disk gap should be three times the thickness of the boundary layer, with a Reynolds number of approximately 10-11[13]. For the 17 krpm rotor, a 0.3 mm disk gap appears to be optimal, showing a peak efficiency of 57.5% at 12 g/s mass flow, with 250 W of power. The rotor-only efficiency at this condition is approximately 80%. At low mass flow rates, there is always a higher rotor efficiency.

3.2. Reversible Tesla machine in expander mode

In this section, the performance analysis of the reversible Tesla machine is presented in expander (direct) mode. As illustrated in Figure 6 (I), the expansion ratio (ε) of the expanders at 22 krpm and 17 krpm is plotted against the mass flow rate: total to static expansion ratio (ε) is defined as reciprocal of the total to static pressure ratio, defined in eq. (1). As discussed in sections 2 and 3.1, the optimal disk gap in compressor mode is 0.3 mm at 17 krpm, but it may differ from the optimal gap for expander mode, which has not been calculated yet. However, only 0.3 mm gap is considered for both angular speeds of 17 krpm and 22 krpm, since that will be the prototype actual gap. The expansion ratio (ε) increases linearly with increasing mass flow rate regardless of the angular speed, but 22 krpm has a higher ε than 17 krpm. This is possible due to rotational speed. At the peaks efficiency expansion ratios are 1.39 and 1.67 for 17 krpm and 22 krpm respectively.

As shown in Figure 6 (II) the total efficiency (solid line) and the power (dashed line) are plotted against mass flow rate. The total to static efficiency and outlet power are calculated by Eq. (4 and 5). Please note that these power and efficiency are evaluated based on the CFD without losses consideration, the experimental will bit differ that considering the losses. For both angular speeds 17 and 22 krpm, the expander efficiency increases linearly as the mass flow rate increases until peak points are reached at 30 g/s and 40 g/s, respectively. For angular speeds 17 and 22 krpm, the efficiency gradually decreases from peak point to increases the mass flow rate. As the flow rate increases, the 22 krpm becomes flatter than the 17 krpm.

$$\eta_{t-st} = \frac{\tau * \omega}{\dot{m} * C_p * T_{t_i} * (1 - 1/(\varepsilon_{t-st}^{(\frac{k-1}{k})}))} \quad (4)$$

$$P_{cfd-out} = \tau * \omega \quad (5)$$

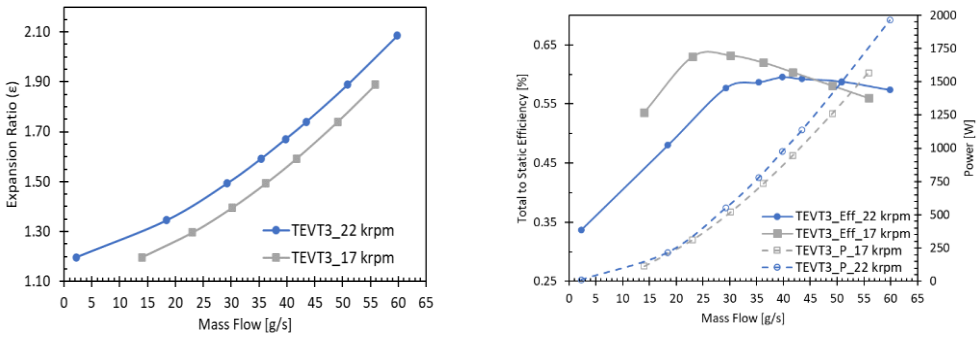

(I) (II)

Figure 6: Reversible Tesla machine in expander (TEVT3) mode: (I) Expansion ratio vs mass flow rate (II) Total to static efficiency (solid line) and power (dashed line) vs mass flow rate.

The total to static peak efficiency at 17 krpm is 63.5% at 30 g/s when inlet pressure is 1.4 bar. The efficiency of 22 krpm is approximately 59.5 percent at 40 g/s with an inlet pressure of 1.68 bar. It has been shown that power increases linearly with increasing mass flow rate for both angular speeds. The power output at peak efficiency is approximately 521 W for 17 krpm and 975 W for 22 krpm. The power curve has almost the same gradient at low mass flow rates, whereas as the mass flow rate increases, the gradient is gradually increasing at 22 krpm as compared to 17 krpm. There is a tendency for the flow angle between corotating disks to try to achieve the best angle for each mass flow rate. If the disk gap is optimal, this tendency could be more pronounced [13][14]. Since the optimal disk gap varies from a compressor to expander design, this study optimized the Tesla rotor for compressor mode only, using the fact that the Tesla expander efficiency curve is flatter than that of the compressor. While this analysis does not take into consideration whole rotor assembly losses, the prototype will also include end wall and mechanical losses, which are expected to significantly reduce overall performance.

4. Conclusion

This work presented the numerical design study of an air Tesla prototype under construction, aiming at reversible operation, i.e. both expander (direct) and compressor (indirect) modes of operation: for this reason, a bladeless rotor has been coupled to a bladeless stator, i.e. a volute type of casing. The rotor has been designed according to compressor optimal performance, and the expander performance has been calculated consequently. In examining the overall efficiency of this Tesla device without taking into account the overall assembly losses (namely end-wall ventilation, end-wall leakage losses and mechanical losses), it is expected to achieve maximum efficiency of 57.5% in compressor mode and 63.5% in expander mode, both at 17kprm nominal speed. Interestingly, the expander mode operation presents peak efficiency at roughly double the nominal mass flow in compressor mode. These results need to be validated through an extensive experimental campaign, already planned in the near future.

Acknowledgements

This project has received funding from the European Union's Horizon 2020 research and innovation programme under the Marie Sklodowska-Curie Grant Agreement No. 861079 ("NextMGT - Next Generation of Micro-Gas Turbines for High Efficiency, Low Emissions, and Fuel Flexibility"). This paper reflects only the authors' view and the Research Executive Agency, and the European Commission are not responsible for any use that may be made of the information it contains.

References

[1] Tesla, N., 1913, "Turbine", US Patent 1061206.
[2] Tesla, N., 1913, "Fluid propulsion" US Patent 1061142.
[3] Tiwari, R., N., Niccolini Marmont, C., A., Reggio, F., Silvestri, P., Traverso, A., and Ferrari, M., L., "Acoustic Signature Analysis of a Bladeless Blower", *Applied Acoustic*,**Vol-208(6)** (2023), https://doi.org/10.1016/j.apacoust.2023.109382.
[4] Mantelli L, Ferrari M.L., Traverso A., "Dynamics and control of a turbocharged solid oxide fuel cell system", *Applied Thermal Engineering*, 191 (2021) 116862_1-14.
[5] Rice, W., 1963, "An Analytical and Experimental Investigation of Multiple Disk Pumps and Compressors", *J. Eng. for Power,* **85(3)** Pp. 191-198, (1963).
[6] Tiwari, R., N., Reggio, F., Renuke, A., Pascenti, M., Traverso, A., Ferrari, M.L.,"Performance Investigation of a Bladeless Air Compressor" *J. Eng. Gas Turbines Power*, **Vol-144(9) (**2022) https://doi.org/10.1115/1.4054945.
[7] Rice, W., "Tesla Turbomachinery," Handbook of Turbomachinery, Logan, E., and Ray, R., Marcel Dekker, New York, Chap. 14 (2003).
[8] Renuke, A, F. Reggio, P. Silvestri, A. Traverso, Pascenti, M.,"Experimental Investigation on a 3 kW Air Tesla Expander with High-Speed Generator", *ASME Turbo Expo 2020*, virtual, ASME Paper GT2020-14572.
[9] Zhao, D., Ji, C., Teo, C., & Li, S., "Performance of small-scale bladeless electromagnetic energy harvesters driven by water or air", *Energy*, 74, 99-108, (2014).
[10] Silvestri, P., Traverso, A., Reggio, F., Efstathiadis, T. "Theoretical and experimental investigation on rotor dynamic behavior of bladeless turbine for innovative cycles" Proceedings of the ASME Turbo Expo, (2019).
[11] http://www.sit-tesla-technologies.com/, last access 14/04/2023
[12] Renuke, A., Reggio, F., Traverso, A., Pascenti, M. "Experimental Characterization of Losses in Bladeless Turbine Prototype" *J. Eng. Gas Turbines Power*, 2022, **144(4),** 041009
[13] Tiwari, R., Eleftheriou, K., Ferrari, M.L., Efstathiadis, T., Traverso, A., and Kalfas, A., "Numerical Investigation of Bladeless Compressor on Different Disk Spaces and Diffuser Configurations" *J. Eng. Gas Turbines Power*, **Vol-145(01) (**2022**).** doi.org/10.1115/1.4055705.
[14] Tiwari, R., N., Traverso, A., Pascenti, M., and Ferrari, M., L., "Performance Investigation of a Bladeless air Compressor Using Numerical Simulation" ASME Turbo Expo 2023, Paper Number GT2023-102615, (2023).